論文 / 著書情報
Article / Book Information

Title	Quadruped Walking Robots at Tokyo Institute of Technology: Design, Analysis, and Gait Control Methods
Author	Shigeo Hirose, Yasushi Fukuda, Kan Yoneda, Akihiko Nagakubo, Hideyuki Tsukagoshi, Keisuke Arikawa, Gen Endo, Takahiro Doi, Ryuichi Hodoshima
Journal/Book name	IEEE Robotics and Automation Magazine, Vol. 16, No. 2, pp. 104-114
発行日 / Issue date	2009, 6
権利情報 / Copyright	(c)2009 IEEE. Personal use of this material is permitted. However, permission to reprint/republish this material for advertising or promotional purposes or for creating new collective works for resale or redistribution to servers or lists, or to reuse any copyrighted component of this work in other works must be obtained from the IEEE.

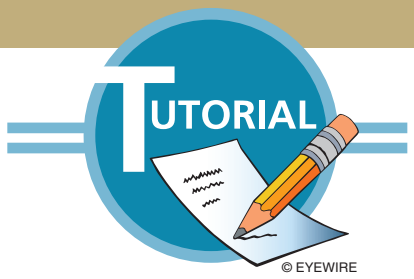

Quadruped Walking Robots at Tokyo Institute of Technology

Design, Analysis, and Gait Control Methods

BY SHIGEO HIROSE, YASUSHI FUKUDA, KAN YONEDA, AKIHIKO NAGAKUBO, HIDEYUKI TSUKAGOSHI, KEISUKE ARIKAWA, GEN ENDO, TAKAHIRO DOI, AND RYUICHI HODOSHIMA

I (Hirose) was walking along a mountain path near Mt. Fuji on a summer day of 1976, when I found a daddy long-legs walking on the ground. I picked it up in my palm and allowed it to walk over my fingers, and the bug walked effortlessly even over finger-made obstacles ten times larger than its own body. While I was watching the motion of the bug, I started to have the desire to make bigger multilegged walking robots, which can walk over large buildings. This was the beginning of our study of walking robots, which was to last for more than 30 years.

The features of a walking robot are as follows: 1) it can move over rugged terrain, and it can step over objects, which should not be damaged without making contact with them, 2) it can realize a holonomic omnidirectional motion without relying on a slipping motion on the ground to minimize the damage to the ground, and 3) it can be a stable and active platform even on a rugged surface in a standstill mode, and its legs can act as manipulators through coordination control. As for the number of legs, we selected quadruped for our basic configuration, as it can secure statically stable walking at slow speed and minimize the mechanical complexity of the actuation system.

Digital Object Identifier 10.1109/MRA.2009.932524

In this article, we will first discuss the design principle of the leg driving mechanism to minimize energy loss and maximize output power. We will also introduce the gait control methods implemented in our previous quadruped walking robots. Finally, we will survey most of the prototype models of our quadruped walking robots.

Design and Analysis of Leg Mechanism

Gravitationally Decoupled Actuation

Because walking robots need to carry an energy source, such as batteries, energy efficiency is one of the most important characteristics. However, walking robots inherently consume a lot of energy because they are driven by many actuators, and furthermore, they have particular processes that cause grave energy loss. Therefore, it is not easy to develop an energy-efficient walking robot, which can walk for a long time to be practical. The gravitationally decoupled actuation (GDA), which we proposed before [1], is the design principle to provide a solution for this problem.

Let us consider walking robots that are walking in the horizontal direction as shown in Figure 1. Here, we assume that the weight of the leg is sufficiently light when compared with that of

1070-9932/09/$25.00©2009 IEEE

the body. During the motion, the leg applies a force $\boldsymbol{F}_b$ to the body in the vertical direction and applies a velocity $\boldsymbol{V}_b$ in the horizontal direction. The direction of $\boldsymbol{F}_b$ and $\boldsymbol{V}_b$ are perpendicular to each other, and so the power (the inner product of $\boldsymbol{F}_b$ and $\boldsymbol{V}_b$) generated by the leg is zero. Here, the power generated by the leg (output power) is equal to the sum of the power generated by the joints that drive the leg (input power). If a joint generates positive power, some other joints surely generate negative power. Focusing on the power generated by the joints of the robot in Figure 1(a), we can find that Joint 1 has an angular velocity v_1 in the counter-clockwise direction and generates a torque f_1 in the clockwise direction, generating negative power $P_1 = v_1 f_1 < 0$, and Joint 2 generates both an angular velocity v_2 and a torque f_2 in the clockwise direction, generating positive power $P_2 = v_2 f_2 > 0$. Now, if a joint generates negative power, it means that the power is supplied to the joint or the joint is used as a brake; however, there are some other joints that supply power to the joint. In this assumed motion, Joint 2 is supplying power to Joint 1 in Figure 1(a). The situation that some joints generate positive power and some other joints generate negative power at the same time is similar to simultaneously stepping on the accelerator and brake of a car. Considering the fact that the power supplied to a joint is dissipated as heat in the actuator that drives the joint, we can see that this situation is obviously unreasonable from the energy efficiency standpoint.

In this assumed motion, the sum of the power generated by the joints is zero, and so the only solution to avoid such an unreasonable situation is to maintain the power generated by every joint at zero. Moreover, to realize this, either the joint-generated velocity (angular velocity) or force (torque) must be zero because the joint-generated power is the product of the joint-generated velocity and force. We call such an actuation state GDA. For a walking robot whose main task is to walk on a ground surface, achieving the state of the GDA is effective in improving energy efficiency.

Figure 1(b) is a typical example of a walking robot designed based on the GDA. Prismatic Joint 1 generates motion of certain velocity with zero force, whereas prismatic Joint 2 generates motion of certain force with zero velocity. Thus, both of the joints generate no power. Therefore, the energy efficiency of the walking robot in Figure 1(b) is higher than that of the walking robot in Figure 1(a). In the "Walking Machine Chronicle" section, we will introduce quadruped walking robots PV-II, TITAN III, and IV designed based on the GDA.

Coupled Drive

Robots, particularly walking robots, have many degrees of freedom (DoF) and must be equipped with many actuators to drive the DoF. However, the power–weight ratios of existing actuators (the maximum output power per unit weight) are extremely low, and the walking robots tend to be heavy in relation to power capability. In the design of walking robots, we often fall into the dilemma that a walking robot designed with an aim to achieve versatile terrain adaptivity is unable to support even its own weight. The coupled drive, which we proposed previously [2], is the design principle to provide a solution for this problem.

Let us consider walking robots that are climbing a vertical wall as shown in Figure 2. Here, we assume that the maximum output powers of the actuators, which drive the prismatic joints, are the same. During the motion, the leg applies both force $\boldsymbol{F}_b$ and velocity $\boldsymbol{V}_b$ to the body in the vertical direction. Therefore, in contrast to the motion assumed in the GDA, a large amount of power is required to achieve the motion. The robot in Figure 2(a) generates this large amount of power only from Joint 1 because Joint 2 generates neither velocity nor force. In other words, this robot can use at most only half of the installed actuator power for the motion. We could say that the actuator, which drives Joint 2, is merely a weight in this motion, deteriorating the performance of the robot. Even if we replace the actuator, which drives Joint 1 with a larger one to provide supplemental power, the effect will be canceled because of the weight increase due to the actuator itself.

We cannot overcome this dilemma simply by increasing the actuator power installed in the robot; instead, we must focus on the effective usage of the installed actuator power. We have already defined the actuation index η_p to evaluate the effective usage [2]

$$\eta_p \equiv \frac{\text{maximum output power for a motion}}{\text{sum of installed actuators power}}.$$

The maximum value of η_p is 1, which means that the robot can use all of the installed actuator power for the motion. The actuation index of the walking robot in Figure 2(a) for the

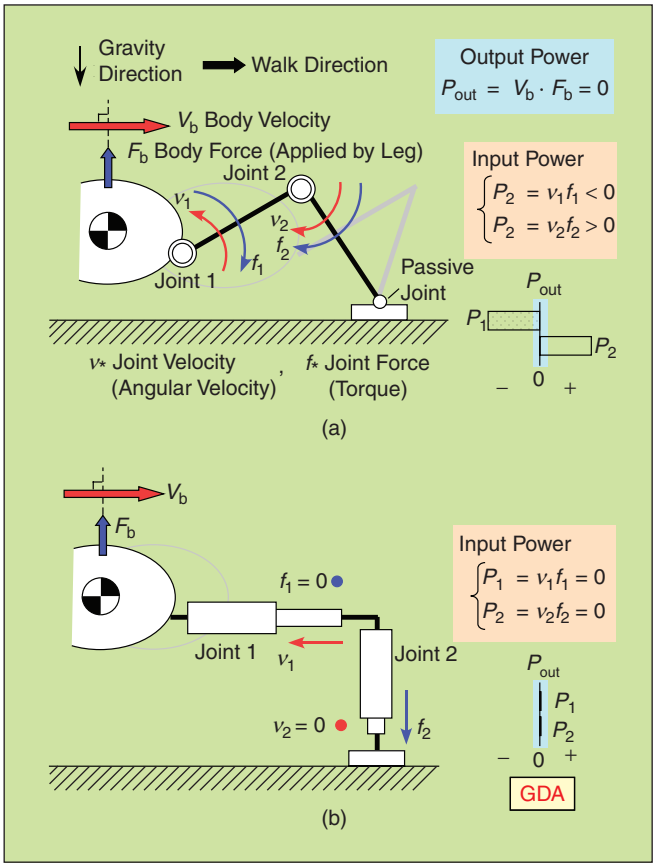

Figure 1. *Gravitationally decoupled actuation: (a) low-energy efficiency and (b) high-energy efficiency.*

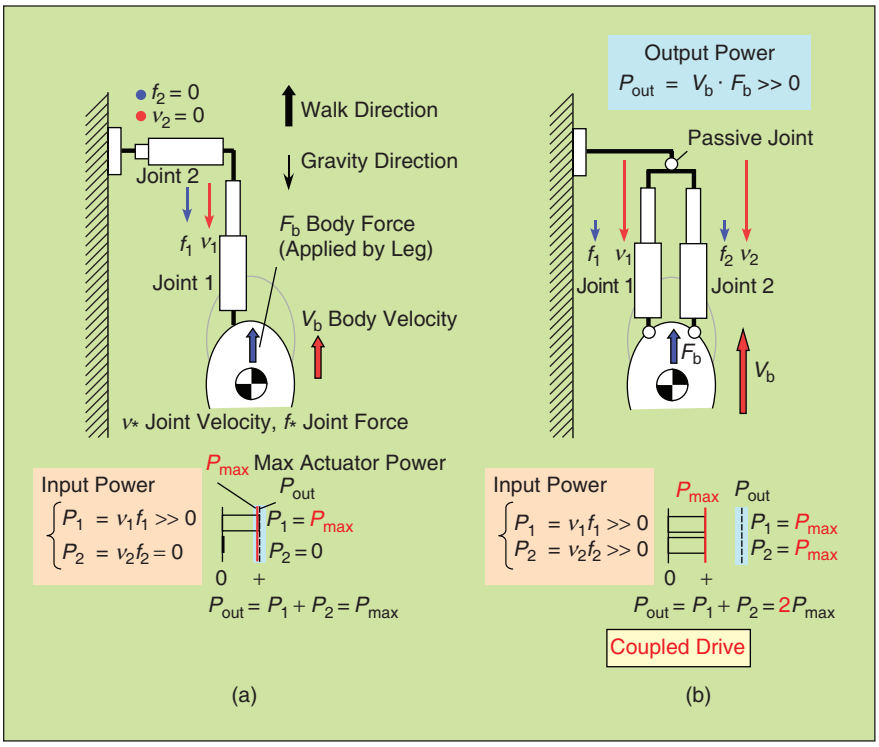

Figure 2. *Coupled drive: (a) low-actuation index and (b) high-actuation index.*

motion is no more than 0.5. Figure 2(b) is a typical example of a wall-climbing–walking robot designed based on the coupled drive. The actuation index of the robot in Figure 2(b) is much higher than that of the robot in Figure 2(a), because both prismatic Joints 1 and 2 generates velocity and force in the same direction, and all actuators evenly provide the required power. Assuming all the maximum output powers of the installed actuators are the same, the weight of the robot in Figure 2(a) and that in Figure 2(b) are similar. Nevertheless, the robot in Figure 2(b) has twice as much power available for the wall-climbing motion. The coupled drive is a design principle to realize compatibility between an increase in DoF and reduction of weight by introducing specific mechanisms and/or control to increase the actuation index as much as possible. In the "Walking Machine Chronicle" section, we will introduce the quadruped walking robots Ninja-I and II designed based on the coupled drive.

Incidentally, it is a requirement that every joint generates zero power in the GDA, so we might feel that the idea of the coupled drive contradicts that of the GDA. However, we should consider these two principles to be very similar rather than contradictory. We can interpret the state in which the GDA is not achieved (i.e., some joints generate positive power whereas other joints generate negative power at the same time) as a state in which the power is concentrated in the joints which generate positive power. Under this interpretation, the GDA state is automatically derived by applying the idea of the coupled drive to the zero power motion such as the motion assumed in Figure 1.

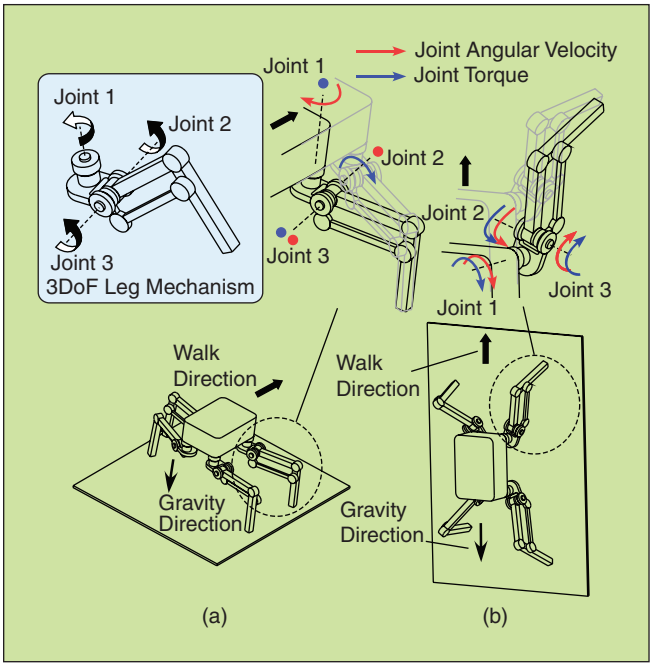

Figure 3. *Selection of walking posture. (a) Ground walk posture: realizing GDA effect; (b) wall climbing posture: realizing coupled-drive effect.*

Selection of a Standard Walking Posture

We have explained that we can realize high performance walking robots by designing the leg mechanisms based on the GDA or the coupled drive. Walking posture can be given as another major factor which influences performance [3].

As shown in Figure 3, let us consider a walking robot that has 3 DoF legs specialized neither to the GDA nor to the coupled drive. Here, we assume that the maximum output powers of the actuators that drive the joints are the same. Figure 3(a) is the walking posture, which realizes the effect of the GDA during ground walking. In this walking posture, Joint 1 generates angular velocity to swing the leg, however, does not have to generate torque to support its own weight. Joint 2 generates torque to support its own weight, however, generates little angular velocity, and Joint 3 generates little angular velocity and little torque. Therefore, every joint generates little power and the condition of the GDA is almost achieved. The walking robot can efficiently walk on the ground in this walking posture by the effect of the GDA. However, if it climbs a wall in the same posture, the performance will not be so good because only Joint 1 provides nearly all the power required for the motion. Figure 3(b) is a walking posture that realizes the effect of the coupled drive. Every joint generates both angular velocity and torque in the same direction, so all joints evenly provide the

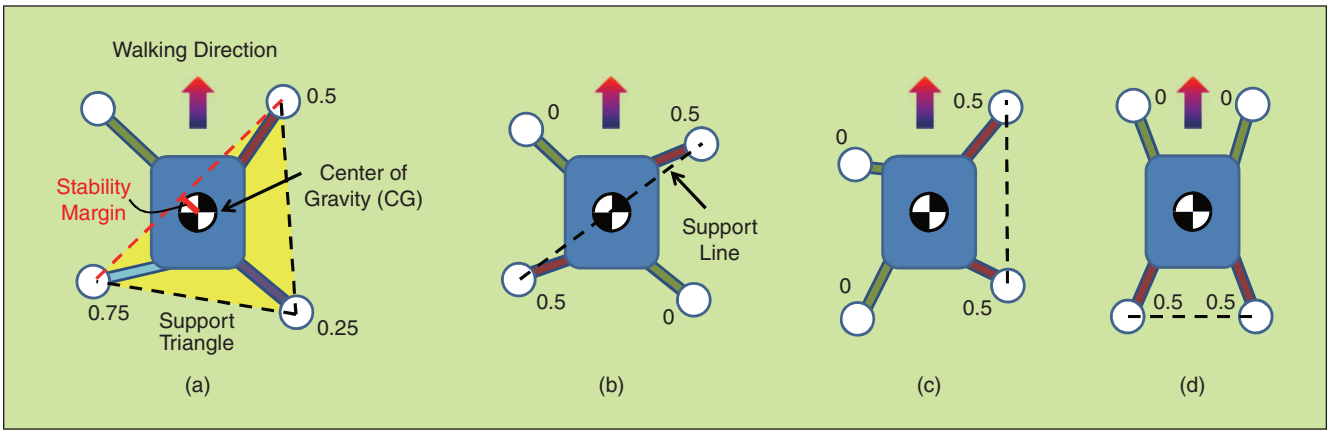

Figure 4. *Typical gait observed in animal locomotion: (a) crawl, (b) trot, (c) pace, and (d) bound.*

required power. In this way, the effect of the GDA or the coupled drive is achieved by walking posture selection as well as mechanism design. In the "Walking Machine Chronicle" section, we will introduce the quadruped walking robot TITAN VIII, which realizes the effect of the GDA through selection of an appropriate walking posture.

Moreover, besides ground walking and wall climbing, there are appropriate walking postures corresponding to various conditions (e.g., steep-slope climbing, high-speed walking, and walking with a heavy load). Adaptively selecting an appropriate walking posture according to the conditions is an effective strategy for maintaining a high-performance walking motion (e.g., selecting the GDA posture during ground walking and the coupled drive posture during wall climbing).

Walking Gait

A gait is a manner of walking of an animal/robot such as an order and timing of swinging the legs, and the duration of the support phase and swing phase. It is generally known that quadruped animals, such as dogs and horses, adaptively change their gaits according to the situation. In this section, we introduce various gaits and discuss their characteristics.

Basics of Gait

Figure 4 illustrates typical gaits of a quadruped animal [4]. The notated numbers indicate the timing of the beginning of the swing phase for each leg within a gait period. For example, the crawl gait lifts the front left leg, the rear right leg, the front right leg, and the rear left leg, in sequential order. The crawl gait is often observed in slow-speed animals, such as a turtle. Here, we introduce a duty factor β, which is the ratio of the durations of the support phase and swing phase [5]. In the case of the crawl gait, $\beta = 0.75$. The total number of supporting legs is always three because $4 \times 0.75 = 3$, indicating that the crawl gait always maintains static stability during walking. Such a gait is called a *static walk*. (Additionally, the crawl gait is categorized as a special case of the forward-wave gait that transfers a swinging leg from the rear to the front.) Stability margin is often used to measure the static stability of a robot [6]. It is the minimum distance between the edges of a supporting polygon and the position of the center of gravity (CG) shown in Figure 4(a).

In contrast with the crawl gait, the other gaits with the usual $\beta < 0.75$ (Figure 4) have a phase where the number of supporting legs is two. This kind of gait requires dynamic balance to continue a steady walk, and is called a *dynamic gait*. Although a dynamic gait does not have stability compared with a static gait, it achieves high mobility at high velocity. The zero moment point (ZMP), which includes the position of the CG, moment of inertia and its dynamic effect by acceleration/deceleration, is often used as an indicator to evaluate dynamic balance [7]. The trot gait and pace gait are observed in a lizard and a camel. A running dog and a horse choose between bounding or galloping, which has a slight phase difference between the left and right legs. It is important to select an appropriate gait depending on the desired walking movement.

Convergence-to-Standard Type Free Gait

A static walk possessing a high-inherent stability is desirable for a relatively slow walking robot on the ground. A steady standard gait is possible in a flat environment. However, in the case of rough terrain where large obstacles and holes exist, it is not necessarily feasible to place the supporting leg in a desirable position. Therefore, a terrain-adaptive gait in a rugged environment is required. We have proposed a convergence-to-standard type free gait [8], which sequentially determines the

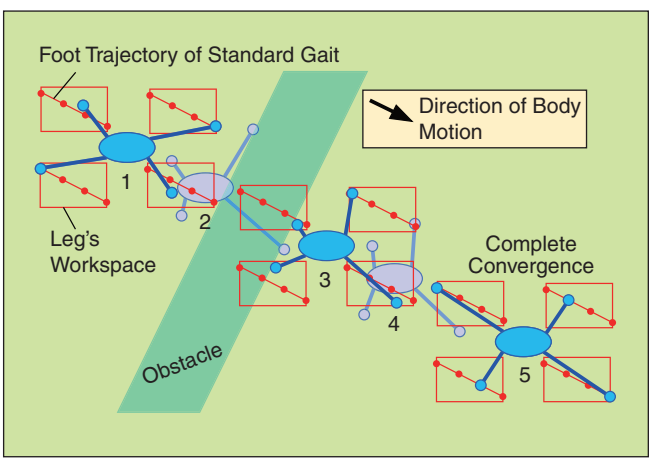

Figure 5. *Convergence to standard gait after negotiating an obstacle.*

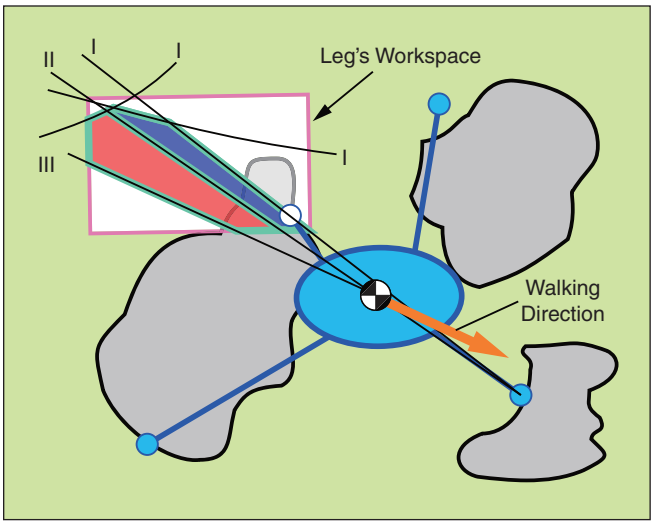

Figure 6. *Domain prescribing method to reduce search space of the next landing point. Green lines bound the possible landing area. Blue area has higher priority and red area has lower priority.*

next step considering continuity of walking, leg workspace, and convergence to the standard gait. Figure 5 illustrates a conceptual image of the gait. Although the standard gait is modified during obstacle avoidance, it converges to the original standard gait after walking over the obstacle.

We chose the crab-walk gait as the standard gait, which is an omnidirectional wave gait with a four-legged supporting phase. The walking step is determined as follows: 1) select the next leg to swing, 2) derive the traveling distance of the CG, 3) set the search space for the landing position of the swinging leg, and 4) determine the landing position.

In Step 1), we focus on the current relative position of the four legs and investigate whether the current leg position even partially matches that of the standard gait. If there is matching part, a leg suitable for continuing the standard pattern is selected without changing the pattern of the matching part. If none of them match, the leg with the longest plane-returning distance is selected.

In Step 2), the moving distance of the CG is determined to provide the robot with a statically stable condition in either the four- or three-legged supporting phase.

Step 3) is composed of three layers named *domain-prescribing method (DPM)-I, II, III* shown in Figure 6. The method aims to ensure continuity of walking. When the next swing leg is a rear leg, DPM-I restricts the landing position to keep the CG inside the supporting triangle considering the succeeding two steps. At the same time, DPM-II provides the priority order with a landing position search in order for the ipsilateral foreleg to be the succeeding swing leg. DPM-II improves convergence to the standard gait. DPM-III restricts the search space to maintain sufficient distance between the left and right legs with respect to the trajectory of the CG.

In Step 4), the initial searching point for the next swing leg is set to the place where the relative phase of each leg is maintained. Then, searching is carried out within the permitted area to determine whether or not the robot can actually land the swing leg using environmental map information or tactile sensors at the tip of the leg with searching movements. The robot keeps searching until an appropriate landing position is found.

This algorithm allows the robot to negotiate rough terrain while adaptively changing the gait. Figure 15 shows a stair-climbing experiment in which environmental information is acquired using tactile sensors.

Intermittent Crawl Gait

In the case of a crawl gait with a small duty factor but still larger than 0.75, the CG is located near the diagonal supporting line when the rear leg becomes the swing leg (Figure 7). Thus, there is a high risk of falling backward at this moment. To avoid this situation, the intermittent crawl gait we proposed in [9], [10] is desirable. This gait is suitable for an application, which places extreme importance on safety such as a construction machine on a steep slope (Figure 20).

The intermittent crawl gait moves the CG of the body only in the four-legged supporting phase. Therefore, the walking velocity is limited and the motion is shaky. However, this gait can maximize static stability. Figure 7 illustrates the comparison between the crawl gait (a) and the intermittent crawl gait (b), showing that the intermittent crawl gait generates a lateral motion to increase static stability.

Applying the intermittent crawl gait to the convergence-to-standard type free gait as the standard gait, the robot can avoid known grid obstacles and follow a specified trajectory in a numerical simulation (Figure 8).

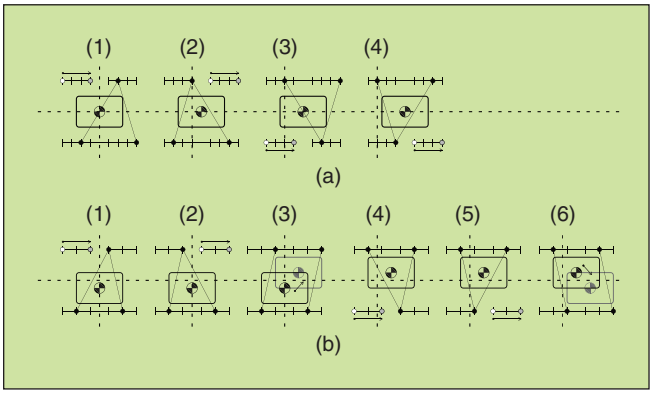

Figure 7. *(a) Crawl gait and (b) intermittent crawl gait.*

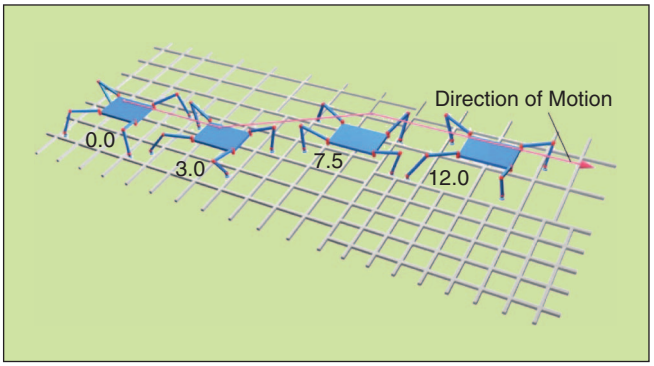

Figure 8. *Simulation of intermittent crawl gait negotiating lattice obstacles.*

Dynamic and Static Fusion Gait

We also investigated a smooth and stable dynamic gait and proposed a dynamic and static fusion gait with sway compensation, which unifies the static crawl gait and dynamic trot gait [11]. In the proposed gait, the swing leg order is the same as in the crawl gait, and the swinging motion of the forward leg starts promptly after touchdown of the rear leg on the same side, and the following swing of the opposite rear leg starts $(\beta - 0.5)T$ later, the swing period being $(1 - \beta)T$, where T is the walking period. As a result, a seamless transition between the crawl gait and trot gait is realized. Also, the gait has a four-legged support phase, which occurs at the moment of touchdown of the rear leg and stabilizes a slight imbalance caused in the two-legged support phase.

Moreover, sway compensation provides a stably balanced trot gait. When standing on two supporting legs, an inverted pendulum is formed around the axis of the diagonal support line, which connects the contact points of the supporting legs and constitutes a zigzag line shown in Figure 9(a). If the ZMP is kept on this line, a stable dynamic trot is achieved because of the moment around the axis being zero. Such a trajectory of the ZMP can be generated by a swaying motion of the CG. Under the condition that the CG $P_g = (x_g y_g z_g)^T$ maintains a constant acceleration in the direction of travel and a constant height, a trajectory of the CG, which satisfies the ZMP $P_{\mathrm{zmp}} = P_g - (z_g/g)\ddot{P}_g$ tracing the diagonal support line, is derived as follows:

$$x_g = x_0 + vt + \frac{1}{2}at^2, \quad z_g = \text{const}, \tag{1}$$

$$y_g = C_1 e^{\frac{t}{\sqrt{A}}} + C_2 e^{-\frac{t}{\sqrt{A}}} + B_2 t^2 + B_1 t + 2AB_2 + y_{z0}, \tag{2}$$

where a, A, B_i and C_i are constants.

Figure 9(b) shows the experiment of the dynamic and static fusion gait with sway compensation by TITAN IV, while continuously shifting the gait from the standstill state to the fully dynamic trot. It illustrates a straight trajectory of the CG in $\beta \geq 0.75$ and an increase in sway compensation in $0.75 \geq \beta \geq 0.5$. We have to notice that the trot gait by the quadruped has an exceptional feature of high reliability, because two swing legs are being swung forward just above the ground on both sides of the diagonal support line, which can be used as stoppers to prevent a full stumble of the body in case the balance of the body is lost. Therefore, even though the trajectory control is not sufficiently precise, we can normally generate the trot gait with ease. Walking on a circular path by TITAN VI [11], [12] and three-dimensional (3-D) sway compensation [13] were also investigated.

Wall Gait: An Optimal Gait on the Wall

After various studies on ground walking, we have developed quadruped wall-climbing robots and investigated an optimal gait on the wall and ceiling from the viewpoint of motion stability and speed [14].

If the robot always keeps three or four legs in the suction state, walking speed is not affected by the swing leg order. However, in the gait that allows two legs in the suction state, a unique balance issue arises. Because of a rotational degree of freedom around the support legs rotation (SLR) axis, which connects the ankles of two suction legs, a moment around the slanted SLR axis is generated by its own weight. This moment rotates the robot and brings it into a failed face-up posture or a stable posture with a swing leg touching the wall. Also, a stable pushing force for the sucking pad is produced by the moment that is useful to increase the sealing capacity of the pad.

On the basis of these factors, we analyzed the gait, which maximizes walking speed, avoids a face-up posture, and generates a stable pushing force. As a result, an optimal gait, wall gait, has been derived, which maintains a foot posture with a Λ shape and a special swing-leg order never used in ground walking. Since the wall gait allows simultaneous execution of sucking and leg swinging, efficient speedy static walking in $\beta = 0.75$ is realized (Figure 10). Moreover, the Λ shaped foot posture enables a dynamic pace gait on the wall, which provides more speedy locomotion.

We knew that the trot gait and the crawl gait are suitable for ground walking, and the wall gait is suitable for wall climbing. As for a gait for the ceiling, we found that the trot is most suitable just as in the case of ground walking. When the walking robot is suspended from the ceiling, supporting the robot with two suction legs and driving the CG along the zigzag connecting lines shown by the solid line in Figure 9 is fastest and most reliable [15].

Roller Walk: A Special Gait for Roller Skating

Equipping a passive wheel at the tip of each leg provides a walking robot with wheeled locomotion similar to roller skating. We named it "Roller-Walk" and investigated the special leg trajectory that generates wheeled propulsion.

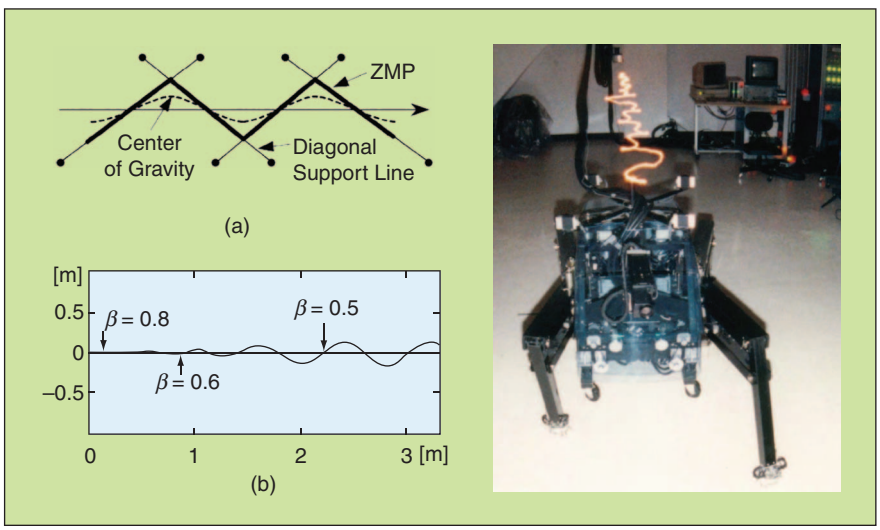

Figure 9. *Stable dynamic and static fusion gait with sway compensation. (a) Sway compensation to keep ZMP on diagonal support lines. (b) Trajectory of the CG with continuous transition of β.*

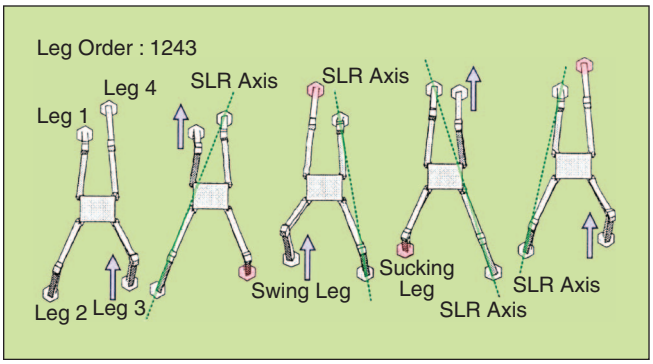

Figure 10. *The wall gait that enables efficient speedy walking on the wall.*

There are infinite possibilities for the leg trajectory within a leg's workspace. To simplify the problem, we assume that 1) all legs are in the support phase, 2) all legs are mass less, and the CG of the robot is located in the middle of the body, and 3) the left and right legs move with a symmetrical periodic motion. Figure 11 shows a coordinate system for numerical analysis. We assume a symmetric leg trajectory as follows:

$$d(t) = d_{\text{offset}} + d_0(\sin(\omega t + 3\pi/2) + 1), \quad (3)$$

$$\theta(t) = -\theta_0 \sin(\omega t + 3\pi/2 + \varphi), \quad (4)$$

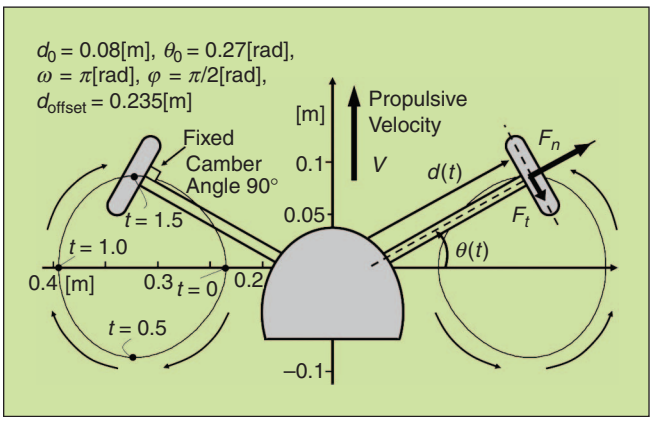

Figure 11. *Roller-walk: skating gait using passive wheels.*

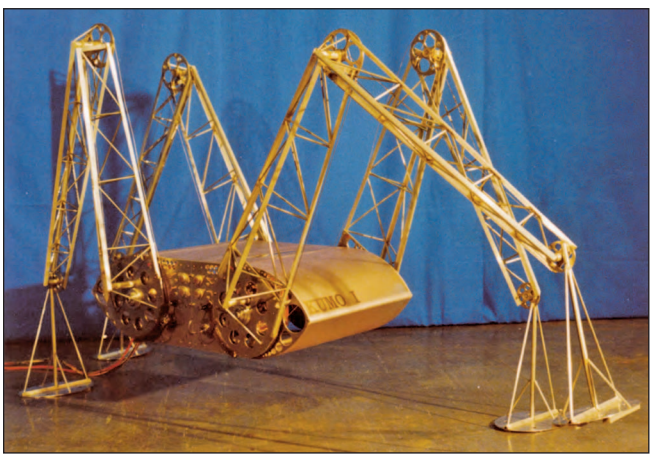

Figure 12. *KUMO-I: the first prototype developed in 1976.*

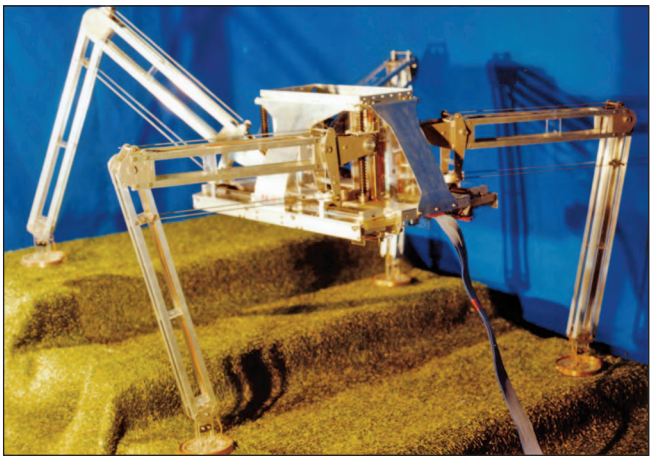

Figure 13. *PV-II second generation, developed in 1977–1979.*

where parameters d_0 and θ_0 are the amplitudes of sinusoidal oscillation in the normal and tangential directions of the passive wheel, respectively. ω determines the angular velocity of the oscillations. φ is the phase difference between the oscillations in the normal and tangential directions. We can optimize the four control

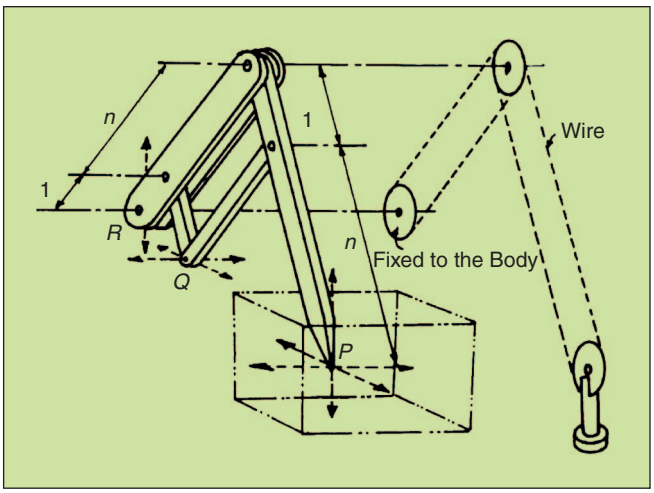

Figure 14. *PANTOMEC: 3-D pantagraphic mechanism enlarges leg's workspace.*

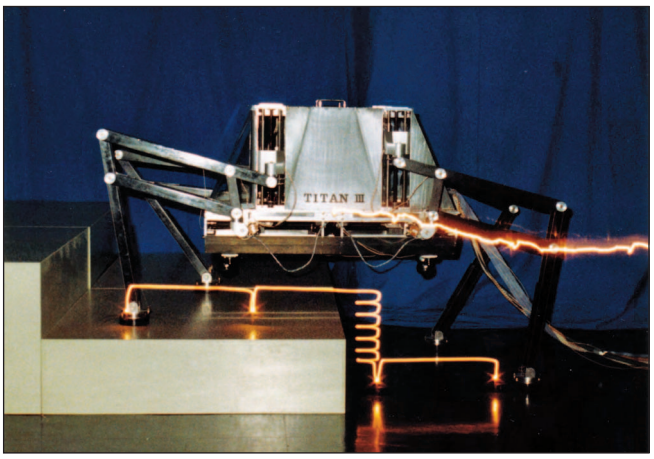

Figure 15. *TITAN III climbing up stairs using tactile sensors.*

parameters, d_0, θ_0, ω, φ, to obtain a maximum propulsive velocity. An example of the leg trajectory is illustrated in Figure 11.

We confirmed that the propulsive velocity is proportional to ω, and that the propulsive direction is controlled by adding a steering offset to $\theta(t)$. The maneuvering of the robot motion can be very similar to an ordinary car [16].

Walking Machine Chronicle

In this section, we briefly introduce in chronological order the walking robots that we have developed so far. More detailed information can be found in the references.

KUMO-I is the first prototype model of our walking robot inspired by a daddy long-legs in 1976 [17]. The leg length is 1.5 m, and the weight of the robot is 14 kg (Figure 12). KUMO-I has 8 DoF to perform walking in the sagittal plane. However, each leg has only one actuator and uses a clutch mechanism to reduce the total weight of the robot. Locomotion ability is insufficient because of the limited power of the actuator. The results suggest that straightforward mimicking of animals is not effective to develop a walking robot. This experience leads to the proposal of the GDA concept.

PV-II is the second prototype with the GDA concept (Figure 13) [18]. The leg length is 0.9 m, and the weight of the robot is 10 kg. The originally proposed 3-D pantagraphic mechanism (PANTOMEC) [19] shown in Figure 14 was adopted to increase the leg's workspace and reduce the weight of the leg. This mechanism expands the prismatic motion of the three orthogonal axes provided on the torso part and simplifies their control. In 1979, the PV-II was the world's first success in sensor-based stair climbing using leg-end tactile sensors and posture sensors.

TITAN III has improved on the PANTOMEC legs with an increased mobility range and reduced weight by using carbon fiber composite plastic (CFRP) [8]. The length of the legs is 1.2 m, and the weight of the robot is 80 kg (Figure 15). The feet of TITAN III are equipped with whisker sensors and a signal processing system that is made up of wires with shape memory alloy properties that have hyperelastic characteristics and measure the status of ground contact. Moreover, the robot is also equipped with a posture sensor, and is loaded with an intelligent gait control system called perspective gait supervisory system (PEGASUS) for the purpose of making decisions regarding the sensor information in an integrated manner and realizing terrain-adaptive static walking.

TITAN IV was displayed at the Government Pavilion of the science exhibition in Japan, in 1985, and walked a total of approximately 40 km by continuing a round-trip across a stage that had three different step levels, as shown in Figure 16, during the half-year exhibition period. In addition, it also realized a static and dynamic fusion gait [11]. TITAN IV walked with a velocity of up to 0.4 m/s, and the length of the legs is 1.2 m, whereas the weight of the robot is 160 kg.

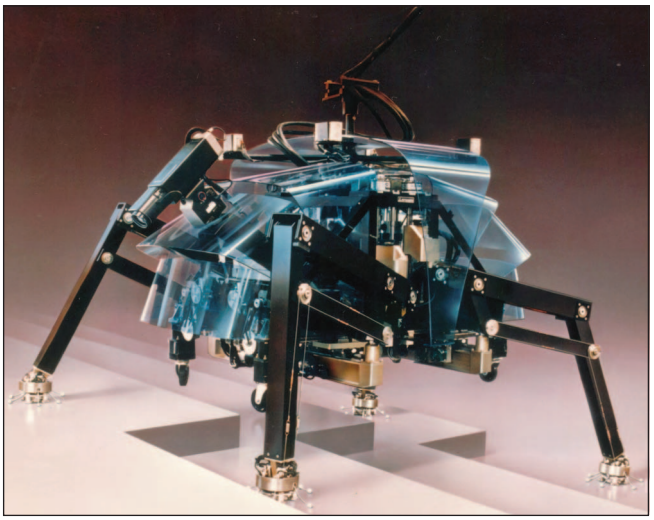

Figure 16. *TITAN IV demonstrated at the science exhibition in 1985.*

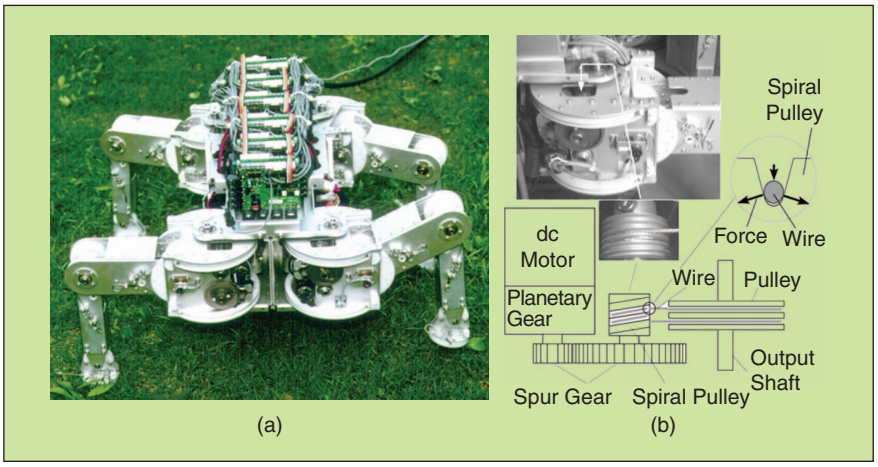

Figure 17. *(a) TITAN VIII and its joint driving mechanism (b) with spiral pulleys and wire.*

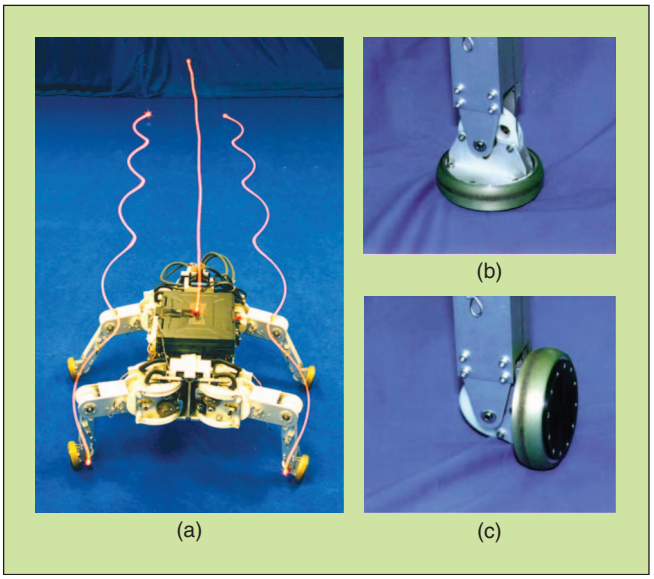

Figure 18. *Roller walker: (a) the white lines show trajectories of the frontal leg ends and the body. (b) Walking mode and (c) skating mode.*

For a walking robot whose main task is to walk on a ground surface, achieving the state of the GDA is effective in improving energy efficiency.

TITAN VIII was developed as a research platform enhancing the walking robot study funded by a governmental project. The length of the legs is 0.4 m, and the weight of the robot is 22 kg (Figure 17) [20]. The walking velocity and payload are 0.2 m/s and 7 kg, respectively. The most challenging issue in mechanical design is to reduce the production cost so as to commercialize the robot at a reasonable price for researchers. Therefore, we chose simple revolute joints for the leg mechanism and performed the GDA concept by selecting an appropriate walking posture. Moreover, we constructed the structural parts of the robot using sheet metal and bending processes as much as possible.

One of the notable mechanisms of this leg is the use of wire and a spiral pulley driving system [Figure 17(a)]. In this system, when the wire is stretched to some extent, the wire digs into a V-shaped groove. The wire is strongly pressed against the surface of the V-shaped groove (wedge effect), and this effect supports a large tangential force. This effect permits the actuator to transmit sufficient torque to perform walking, which usually generates a large impulsive reaction torque. TITAN VIII was successfully commercialized by TOKYO SEIKI Co., Ltd., at the price of US$15,000, and more than 75 robots have been sold to researchers in Japan.

Roller Walker is a leg-wheel hybrid robot with passive wheels, which can be transformed into a walking mode and a skating mode by rotating an ankle roll joint at a right angle [16] [Figure 18(b) and (c)]. Roller Walker performs wheeled locomotion with the same principle of roller skating, while using the leg's actuators for walking. This concept is highly related to a coupled drive in terms of actuator-operating ratio. Roller Walker can also minimize the weight of the walking robot by hybridization, because a passive wheel is the simplest and lightest type of wheel.

The sole disk is always mechanically kept parallel to the body by a parallel-link mechanism with a wire–pulley system. The ankle roll joint is controlled by driving the wire with a small actuator with respect to the leg's base structure.

We experimentally verified a maximum velocity of 2.3 m/s, which was 11 times faster than the walking velocity [21], and the efficiency of locomotion was eight times higher than that of the crawl gait.

Ninja-I and *II* are wall-climbing robots developed in 1990–1993 and 1994–1998, respectively. They were developed based on the actual needs for several operations on the walls of buildings and plants, such as inspection and maintenance. Key points of this study are leg mechanisms based on coupled drive, optimized gaits on the wall and ceiling, and the ability of 3-D locomotion. Ninja-I is the first robot to which the concept of coupled drive was straightforwardly applied. It has the leg mechanism, which is the 3-D-extended one illustrated in Figure 2(b) by using three linear actuators, and newly developed valve-regulated multiple (VM) suction pads, which consist of many compact vacuum

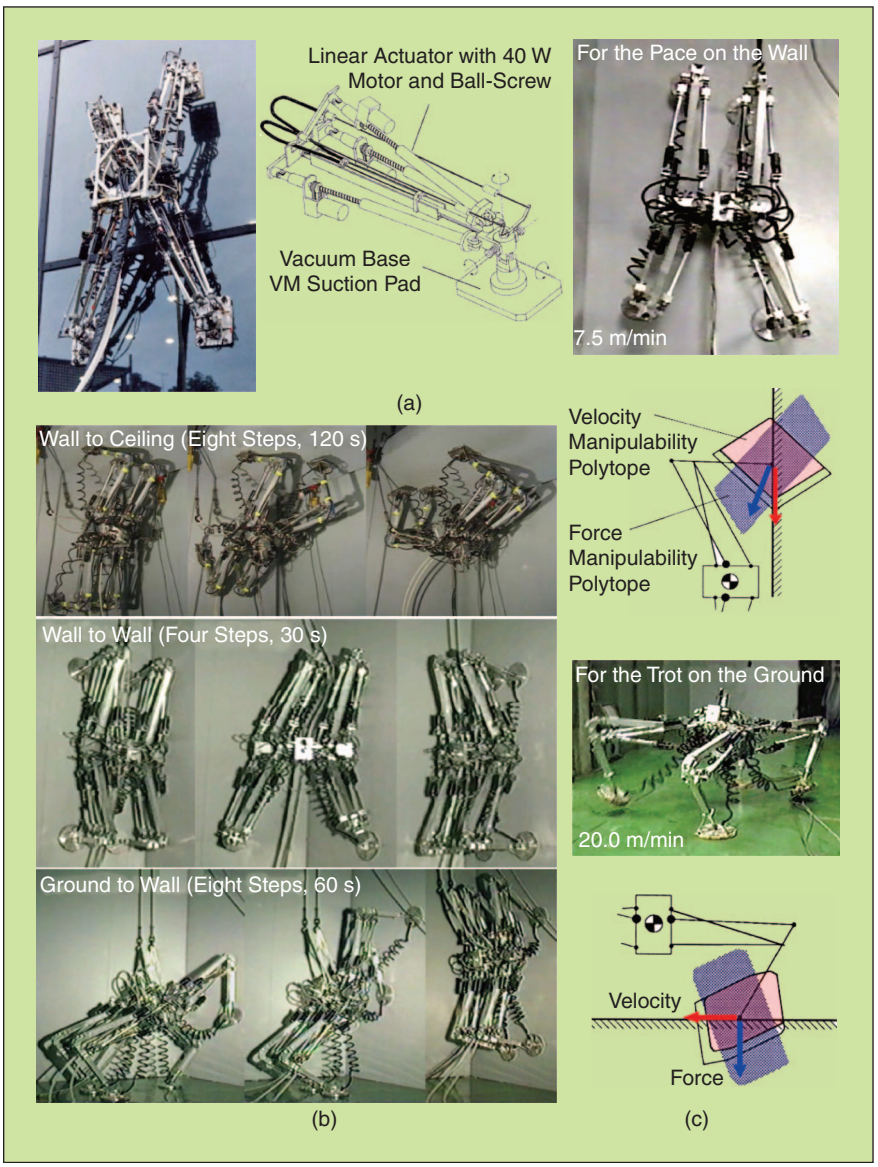

Figure 19. *Quadruped wall-climbing robots Ninja-I and Ninja-II. (a) Ninja-I and its coupled drive base leg mechanism. (b) 3-D locomotion of Ninja-II. (c) Manipulability polytopes optimized for dynamic walking.*

suckers with passive valve mechanisms to avoid vacuum leaks by cracks or ditches [22] [Figure 19(a)].

In the design of Ninja-II, not only wall climbing but also dynamic walking on the ground and wall, and more extended 3-D locomotion were considered. To realize both the coupled drive and a wide reachable area, a parallel-driven serial link mechanism was introduced. The leg characteristics are determined based on a manipulability polytope, which provides a most basic way to design the coupled drive [23] [Figure 19(c)].

Ninja-I achieved walking on the wall (wall gait, 0.8 m/min), ground (crawl, 0.8 m/min), and 3-D environment (wall-to-wall, 40 s). Ninja-II performed walking on the wall (wall gait, 3.0 m/min; pace, 7.5 m/min), ceiling (trot, 5.0 m/min), ground (trot including a sideway and turning gait, 20 m/min), and 3-D environments (floor-to-wall, 60 s; wall-to-wall, 30 s; wall-to-ceiling, 120 s) [15], [23].

Both of the Ninjas have a length of 1.8 m, weight of 45 kg, 12 40-W motors, and vacuum suckers with a sucking force of 120 kgf.

TITAN XI was developed for a drilling task on a sloping construction site (Figure 20). The length of the legs is 3.7 m, and the weight of the robot is 7,000 kg [24]. To the best of our knowledge, TITAN XI is the largest quadruped in the world. The legs are driven by hydraulic cylinders, and a drill is mounted in the middle of the body. Two winches are installed on the back to reel tethers to assist in climbing a slope.

In the process of development, we made two prototypes of the leg mechanism shown in Figure 21 and compared their performances. The coupled-drive leg mechanism has a high-load capacity and large workspace, thus being an appropriate leg mechanism for walking on undulated ground. However, it required a comparatively long cylinder stroke and high-mechanical stiffness for a heavy load, increasing the weight of each leg system. The back-hoe-modified mechanism had reduced power output at the tip of the leg and a smaller workspace for walking, but it could still support half of the weight of TITAN XI while weighing less. Moreover, it had enough workspace above the main body for the motion of raising its foot high, a necessity for the transition from flat ground to a steep slope. We concluded that the specification of the back-hoe-modified mechanism satisfied the requirements for construction tasks on the steep slope.

TITAN XI had already succeeded in climbing up a test slope imitating an undulated construction site by avoiding contact with the ferroconcrete frame by using a vision system and gait based on the intermittent crawl gait. An experiment of a drilling task on a 70° slope in a real construction site was also successfully performed.

Currently, we are working on an automatic control system for the drilling and moving tasks and are also improving the manual control system to increase the usability of the robot as a practical tool.

Conclusion

Inspiration from the walking motion of the a daddy long-legs has kept us motivated to create a series of quadruped walking robots and has given us the opportunity to think of the fundamental principles behind the design and control of leg driving mechanisms and gait control for off-the-road ground walking, steep slope climbing, and wall climbing. However, our study is still ongoing [25], and we hope to report on the continuation of this research in the near future.

Figure 20. *TITAN XI climbing up a test slope.*

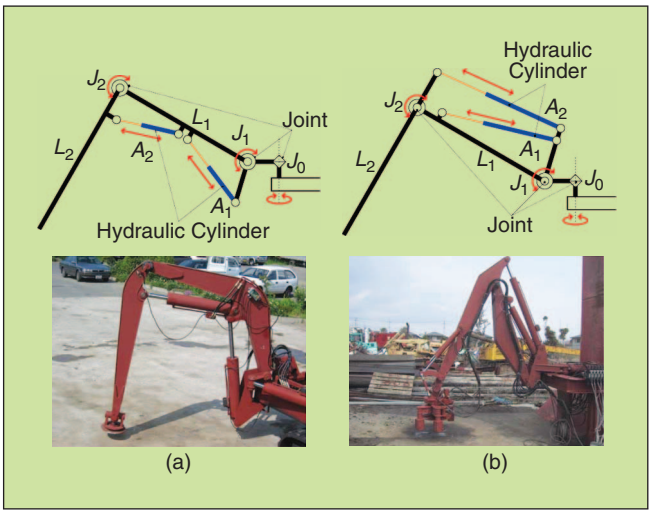

Figure 21. *Prototypes of leg mechanism with hydraulic cylinders: (a) Back-hoe-modified mechanism and (b) coupled drive mechanism.*

Acknowledgments

We would like to express our deepest appreciation to the following former students for their contribution in these research projects: Hiroyuki Iwasaki, Matsuo Nose, Hidekazu Kikuchi, Kazuyuki Masui, Kazuhito Yokoi, Hiroyuki Iiyama, Keisuke Kato, Kazuyosi Kawabe, Masaru Ogata, and Shingo Yokota.

Keywords

Quadruped walking robot, gravitationally decoupled actuation (GDA), coupled drive, gait control.

References

[1] S. Hirose, M. Nose, H. Kikuchi, and Y. Umetani, "Adaptive gait control of a quadruped walking vehicle," in *Proc. 1st Int. Symp. Robotics Research MIT Press*, 1984, pp. 253–277.

[2] S. Hirose and M. Sato, "Coupled drive of the multi-DoF robot," in *Proc. Int. Conf. Robotics and Automation*, 1989, pp. 1610–1616.

[3] K. Arikawa and S. Hirose, "Mechanical design of walking machines," *Philosoph. Trans. R Soc. A*, vol. 365, no. 1850, pp. 171–183, 2007.

[4] B. Siciliano and Oussama Khatib, Eds., *Springer Handbook of Robotics*. New York: Springer-Verlag, 2008, pp. 378–383.
[5] S. Song and K. J. Waldron, *Machines That Walk: The Adaptive Suspension Vehicle*. Cambridge, MA: MIT Press, 1988.
[6] R. B. McGhee and A. A. Frank, "On the stability properties of quadruped creeping gaits," *Math. Biosci.*, vol. 3, no. 3/4, pp. 331–351, 1968.
[7] M. Vukobratovic and J. Stepanenko, "On the stability of anthropomorphic systems," *Math. Biosci.*, vol. 15, pp. 1–37, 1972.
[8] S. Hirose, Y. Fukuda, and H. Kikuchi, "The gait control system of a quadruped walking vehicle," *Adv. Robot.*, vol. 1, no. 4, pp. 289–323, 1986.
[9] H. Tsukagoshi and S. Hirose, "Intermittent crawl gait for quadruped walking vehicles on rough terrain," in *Proc. 1st Int. Symp. Climbing and Walking Robots*, 1998, pp. 323–328.
[10] H. Tsukagoshi, S. Hirose, and K. Yoneda, "Maneuvering operations of a quadruped walking robot on a slope," *Adv. Robot.*, vol. 11, no. 4, pp. 359–375, 1997.
[11] K. Yoneda and S. Hirose, "Dynamic and static fusion gait of quadruped walking vehicle on winding path," in *Proc. Int. Conf. Robotics and Automation*, 1992, pp. 143–148.
[12] S. Hirose, K. Yoneda, K. Arai, and T. Ibe, "Design of prismatic quadruped walking vehicle TITAN VI," in *Proc. Int. Conf. Advanced Robotics*, 1991, pp. 723–728.
[13] R. Kurazume, A. Byong-won, K. Ohta, and T. Hasegawa, "Experimental study on energy efficiency for quadruped walking vehicles," in *Proc. Int. Conf. Intelligent Robots and Systems*, 2003, pp. 613–618.
[14] A. Nagakubo and S. Hirose, "Walking and running of the quadruped wall-climbing robot," in *Proc. Int. Conf. Robotics and Automation*, 1994, pp. 1005–1012.
[15] S. Hirose and K. Kawabe, "Ceiling walk of quadruped wall climbing robot NINJA-II," in *Proc. Int. Symp. CLAWA*, 1998, pp. 143–147.
[16] G. Endo and S. Hirose, "Study on roller-walker (multi-mode steering control and self-contained locomotion)," in *Proc. Int. Conf. Robotics and Automation*, 2000, pp. 2808–2817.
[17] S. Hirose and Y. Umetani, "Some consideration on a feasible walking mechanism as a terrain vehicle," in *Proc. 3rd RoManSy Symp.*, 1978, pp. 357–375.
[18] S. Hirose and Y. Umetani, "The basic motion regulation system for a quadruped walking vehicle," in *Proc. ASME Publication 80-DET-34*, 1980, pp. 1–6.
[19] S. Hirose and Y. Umetani, "A Cartesian coordinates manipulator with articulated structure," in *Proc. 11th Int. Symp. Industrial Robots*, 1981, pp. 603–609.
[20] K. Arikawa and S. Hirose, "Development of quadruped walking robot TITAN VIII," in *Proc. Int. Conf. Intelligent Robots and Systems*, 1996, pp. 208–213.
[21] G. Endo and S. Hirose, "Study on roller-walker—Adaptation of characteristics of the propulsion by a leg trajectory," in *Proc. Int. Conf. Intelligent Robots and Systems*, 2008, pp. 1532–1537.
[22] S. Hirose, A. Nagakubo, and R. Toyama, "Machine that can walk and climb on floors, walls and ceilings," in *Proc. Int. Conf. Advanced Robotics*, 1991, pp. 753–758.
[23] A. Nagakubo, "A study on mechanisms and control of quadruped wall climbing robots," (in Japanese), Ph.D. dissertation, Tokyo Inst. of Technology, Tokyo, 1995.
[24] R. Hodoshima, T. Doi, Y. Fukuda, S. Hirose, T. Okamoto, and J. Mori, "Development of a quadruped walking robot TITAN XI for steep slope operation step over gait to concrete frames on steep slopes," *J. Robot. Mechatron.*, vol. 1, no. 19, pp. 13–26, 2007.
[25] Hirose-Fukushima Laboratory, Tokyo Institute of Technology. (2009). [Online]. Available: http://www-robot.mes.titech.ac.jp/home_e.html

Shigeo Hirose received his doctoral degree in control engineering from Tokyo Institute of Technology in 1976. He is a Fellow of the IEEE. His research interests include design and control of snake-like robots, walking robots, wheels and crawler vehicles, omnidirectional robots, wall-climbing robots, planetary exploration robots, and devices for control of robots. He received the Pioneer in Robotics and Automation Award from the IEEE Robotics and Automation Society in 1999.

Yasushi Fukuda received his doctoral degree in mechanical and aerospace engineering from Tokyo Institute of Technology in 2004. He is a professor of mechanical systems at Tamagawa University. His research interests include walking robots and communication robots.

Kan Yoneda received his doctoral degree in mechanical engineering science from Tokyo Institute of Technology in 1992. He is currently a professor at Chiba Institute of Technology. His research interests include the design of biped, quadruped, hexapod, and leg-wheel hybrid vehicles.

Akihiko Nagakubo received his doctoral degree in mechanical science and engineering from Tokyo Institute of Technology in 1995. From 1995, he has been a research scientist in Intelligent Systems Division, National Institute of Advanced Industrial Science and Technology (former Electrotechnical Laboratory), Japan. His research interests include control and mechanism of physically interactive robots.

Hideyuki Tsukagoshi received his doctoral degree in control engineering from Tokyo Institute of Technology in 1998. His research interests include fluid-powered robotics, rescue robots, and flexible actuators for medical applications. He received the Young Scientists Award from the Ministry of Education, Japan, in 2007.

Keisuke Arikawa received his doctoral degree from Tokyo Institute of Technology in 2000. He is a member of American Society of Mechanical Engineers (ASME). Currently, he is an associate professor at Department of Mechanical Engineering of Kanagawa Institute of Technology. His research interests include the area of analysis and synthesis of multi-DoF mechanisms.

Gen Endo received his doctoral degree in mechanical science and engineering from Tokyo Institute of Technology in 2000. He is an assistant professor at Tokyo Institute of Technology. His research interests include mechanical design, walking robots, leg-wheel hybrid robots, and biologically inspired robots.

Takahiro Doi received his doctoral degree in control engineering from Tokyo Institute of Technology in 2003. His research interests include the area of legged robots and visual sensing.

Ryuichi Hodoshima received his doctoral degree in mechanical and aerospace engineering from Tokyo Institute of Technology in 2006. His research interest includes walking robots.

Address for Correspondence: Shigeo Hirose, Department of Mechanical and Aerospace Engineering, 2-12-1 Ookayama, Meguro-ku, Tokyo 152-8552, Japan. E-mail: hirose@mes.titech.ac.jp.